Supplement of Atmos. Chem. Phys., 26, 4479–4487, 2026
https://doi.org/10.5194/acp-26-4479-2026-supplement

Atmospheric Chemistry and Physics
Open Access
EGU

Supplement of

NH_3 converts Criegee intermediates to nitrogenous organics

Xiaoying Li et al.

Correspondence to: Long Jia (jialong@mail.iap.ac.cn)

Supplementary material: Additional materials, methods, calculation details and experimental data, including photographs of experimental setup.

Structural diagram:

Figure S1 is the structures of Criegee intermediates and several other key species discussed in the manuscript.

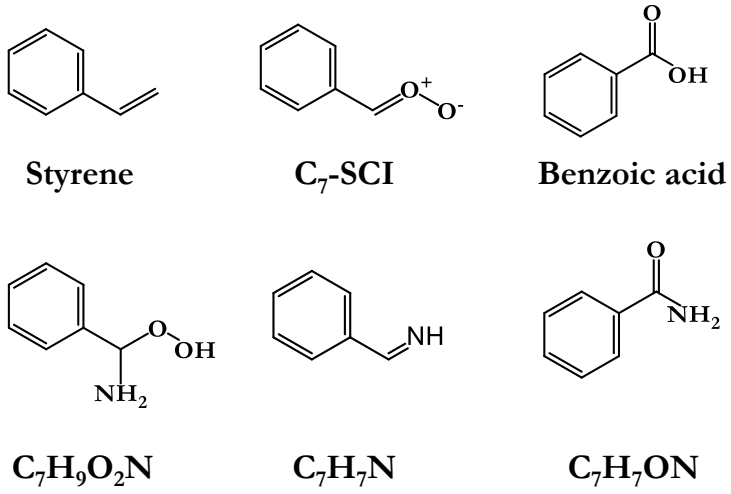

Figure S1. The structures of the key species

Additional materials and methods in experiments:

All the experiments were conducted in FEP reactors (200A, DuPont) under dark conditions. Background air was prepared by Zero Air Supply and CO Reactor (Model 111 and 1150, Thermo Scientific) and further purified by hydrocarbon traps (BHT-4, Agilent). An annular glass denuder was used to remove potentially interfering alkaline gases (URG-2000-30-242-3CSS, Brechtel). The denuder was coated with a solution prepared by 2% phosphoric acid in a solution of 100 mL of deionized water, 4 mL of glycerol, and 150 mL of methanol (Jia et al., 2023; Li et al., 2024; Yu et al., 2024a, b).

Styrene(≥99%, Sigma-Aldrich) was injected into the reactor with zero air using a glass microsyringe, O_3 was produced by an ozone generator (LT 100, LTIAN) with pure O_2(99.995 %, Beijing Huayuan Gas Chemical Industry), and NH_3 (505 ppm in N_2, Beijing Nanfei Gas Company) was directly injected into the reactor. Because ozonolysis of styrene can form OH radicals, n-Hexane was used as an OH radical scavenger (>100ppm). NH_3 concentrations were obtained based on the volume of NH_3 standard gas introduced into the chamber.

The particles from Experiments 1-5 and 11 were collected on a 25 mm polytetrafluoroethylene membrane with a pore size of 0.45 μm (Sartorius stedim biotech Gmbh). The sample flow rate was about 6 L/min and lasted for 40 min. The collected SOA samples were extracted into a 0.5 mL polypropylene vial with pure methanol (Optima™ LC/MS Grade, Fisher Chemical).

Experiments 6-10 were performed with higher concentrations in a 150 L chamber. During these experiments, the products were online ionized by a gas aerosol in-situ ionization source (GAIS), and then measured by Orbitrap MS in the gas phase. The initial conditions are listed in Table S1.

Table S1 Experimental condition

Num.	Styrene /ppm	O_3 /ppm	NH_3 /ppm	Temp. /℃	RH /%
1	0.34	1	0	22.6	6.3
2	0.35	1	0.08	24.0	5.6
3	0.35	1	0.2	24.9	6.3
4	0.33	1	0.4	23.4	6.4
5	0.36	1	0.8	23.1	6.4
6	0.7	2	0.8	19.4	12.0
7	0.7	2	1.8	22.1	15.4
8	0.7	2	1.7	22.2	16.7
9	0.7	2	0	\	\
10	0.4	2	10	19.8	2.1
11	3	10	0.8	10.0	6.0

Iodometry kinetic experiments:

For Experiment 11, the particles were collected on a 25 mm PTFE membrane filter. The collected SOA sample was immediately extracted by 400μL acetonitrile (ACN) before being injected into HPLC-HRMS. Using ACN as extraction solvent to minimize other unwanted decomposition processes such as hydrolysis.

One aliquot (180 μL) from the combined extract mixed with 10 μL acetic acid (600 mM in ACN) in a vial, followed by the addition of 10 μL KI (99.5%, Sigma-Aldrich) (400 mM in H_2O) to trigger the iodometry reaction; another 180 μL aliquot was treated in a same way by adding 10 μL acetic acid (600 mM in ACN) and 10 μL H_2O, instead of KI. These two SOA samples are designated as KI-treated and non-treated respectively, which were injected into HPLC-HRMS (Li et al., 2025).

Parameters for HPLC operation: The Column temperature was set to 35 °C and the injection volume is 1 μL. Mobile phase A is H_2O and B is methanol, the flow rate is 0.2 mL/min. Gradient elution was performed by changing the percentage of mobile phase B over time: 0-2 min:5% B, 22-25min: 100% B, and 27-29min restored 5% B.

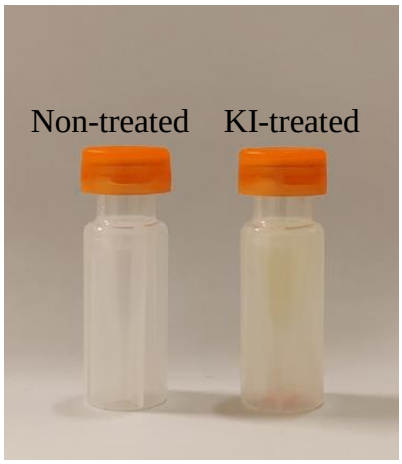

Figure S2: Photo of the Iodometry experiments.

MCM Modeling:

Gas-phase reactions were simulated using the Master Chemical Mechanism (MCM v3.3.1, website: https://mcm.york.ac.uk/MCM) (Bloss et al., 2005; Jenkin et al., 2003), the reaction between NH_3 and C_1-/C_7-SCIs (CH_2OO/PHCHOO) and the subsequent decomposition of $C_7H_9O_2N$ into C_7H_7N and C_7H_7ON was introduced into MCM for simulation:

$CH_2OO+NH_3= CH_2OONH_3$

$PHCHOO+NH_3=PHCHOONH_3$

$PHCHOONH_3= PHCHNH$

$PHCHOONH_3= PHCONH_2$

In addition to the reaction with NH_3, MCM mechanism also includes the following unimolecular and bimolecular reactions of the styrene-derived Criegee intermediates:

$PHCHOO+SO_2=BENZAL+SO_3$

$CO+PHCHOO=BENZAL$

$NO+PHCHOO=BENZAL+NO_2$

$NO_2+PHCHOO=BENZAL+NO_3$

$PHCHOO=BENZAL+H_2O_2$

$PHCHOO=PHCOOH$

$CH_2OO=HCOOH$

$CH_2OO=H_2O_2+HCHO$

$CH_2OO+CO=HCHO$

$CH_2OO+NO=HCHO+NO_2$

$CH_2OO+NO_2=HCHO+NO_3$

$CH_2OO+SO_2=HCHO+SO_3$

Determine the rate constants for the decomposition of $C_7H_9O_2N$ into C_7H_7N and C_7H_7ON:

During the GAIS ionization process, the sample gas is heated to 150 ℃, which significantly increases the decomposition rate of $C_7H_9O_2N$ compared to that at normal temperature (25 ℃). To determine the decomposition rate at 25 ℃, based on the conditions of Exp. 10, we further measured the abundance-time curves of $C_7H_9O_2N$ and its two decomposition products at ionization temperature of 60 ℃. We then added the formation and decomposition reactions of $C_7H_9O_2N$ into the MCM mechanism and adjusted the decomposition rate constants so that the simulated relative proportions of the three substances matched the observed values, thereby obtaining the decomposition rate constants at the two temperatures. The decomposition rate constants of $C_7H_9O_2N$ into C_7H_7N and C_7H_7ON were obtained to be 2.05×10^{-3} s^{-1} and 2.40×10^{-3} s^{-1} at 150 ℃ (1.34×10^{-4} s^{-1} and 2.01×10^{-4} s^{-1} at 60 ℃), respectively. Finally, the decomposition rate constant of $C_7H_9O_2N$ at 25 ℃ was calculated to be 3.0×10^{-5} s^{-1} and 5.1×10^{-5} s^{-1} using the Arrhenius equation.

Toxicity calculation:

The quantitative structure-activity relationship (QSAR) mode is a high-throughput computational toxicology method to predict the environmental exposure and hazard parameters of chemicals. This study used the OECD QSAR Toolbox (Version 4.7, http://qsartoolbox.org) for genotoxicity prediction, and the prediction method was executed according to the workflow in the OECD user manual.

Cramer classification is a toxicity grading tool based on chemical structure decision trees, which classifies substances into low, medium, and high toxicity categories based on structural features such as functional groups and metabolic pathways. It is widely used for safety assessment in food, cosmetics, and other fields, and is continuously updated and optimized with the progress of toxicology research(Cramer et al., 1976).

Table S2 Toxicity calculation results from OECD QSAR

Molecular formula	Cramer classification	Toxicity
$C_7H_6O_2$	I	Low
$C_7H_9O_2N$	III	High
C_7H_7N	III	High
C_7H_7ON	III	High

References

Bloss, C., Wagner, V., Jenkin, M. E., Volkamer, R., Bloss, W. J., Lee, J. D., Heard, D. E., Wirtz, K., Martin-Reviejo, M., Rea, G., Wenger, J. C., and Pilling, M. J.: Development of a detailed chemical mechanism (MCMv3.1) for the atmospheric oxidation of aromatic hydrocarbons, Atmos. Chem. Phys., 2005.

Cramer, G. M., Ford, R. A., and Hall, R. L.: Estimation of toxic hazard—A decision tree approach, Food and Cosmetics Toxicology, 16, 255–276, https://doi.org/10.1016/S0015-6264(76)80522-6, 1976.

Jenkin, M. E., Saunders, S. M., Wagner, V., and Pilling, M. J.: Protocol for the development of the Master Chemical Mechanism, MCM v3 (Part B): tropospheric degradation of aromatic volatile organic compounds, Part B, 2003.

Jia, L., Xu, Y., and Duan, M.: Explosive formation of secondary organic aerosol due to aerosol-fog interactions, Sci. Total Environ., 866, 161338, https://doi.org/10.1016/j.scitotenv.2022.161338, 2023.

Li, K., Zheng, Z., Resch, J., Ma, J., Hansel, A., and Kalberer, M.: Molecular composition of organic peroxides in secondary organic aerosols revealed by peroxide-iodide reactivity, Environ. Sci. Technol., 59, 17126–17136, https://doi.org/10.1021/acs.est.5c03241, 2025.

Li, X., Jia, L., Xu, Y., and Pan, Y.: A novel reaction between ammonia and Criegee intermediates can form amines and suppress oligomers from isoprene, Sci. Total Environ., 956, 177389, https://doi.org/10.1016/j.scitotenv.2024.177389, 2024.

Ma, Q., Lin, X., Yang, C., Long, B., Gai, Y., and Zhang, W.: The influences of ammonia on aerosol formation in the ozonolysis of styrene: roles of Criegee intermediate reactions, R. Soc. open sci., 5, 172171, https://doi.org/10.1098/rsos.172171, 2018.

Yu, S., Jia, L., Xu, Y., and Pan, Y.: Molecular interaction between ammonium sulfate and secondary organic aerosol from styrene, Sci. Total Environ., 954, 176414, https://doi.org/10.1016/j.scitotenv.2024.176414, 2024a.

Yu, S., Jia, L., Xu, Y., and Pan, Y.: Oligomer formation from cross-reaction of Criegee intermediates in the styrene-isoprene-O_3 mixed system, Chemosphere, 349, 140811, https://doi.org/10.1016/j.chemosphere.2023.140811, 2024b.

Experimental data

The data supports the results of all figures.

Table S3 SOA yields under different concentrations of NH_3. (Fig.1a)

NH_3 concentration / ppm	SOA yield / %
0	4.9 ±0.3
0.08	4.3 ±0.3

0.2	3.8 ± 0.2
0.4	2.4 ± 0.2
0.8	1.0 ± 0.1

Table S4 MS data with a relative abundance in the top 90% in positive ion mode. (Fig.1b)

0 ppm NH_3		0.4 ppm NH_3	
m/z	intensity	m/z	intensity
50.421	4.62E+02	51.275	5.80E+02
87.045	2.92E+06	87.045	2.09E+06
103.039	3.14E+06	103.039	2.31E+06
105.055	3.10E+06	105.055	3.16E+06
107.049	6.41E+06	107.049	5.57E+06
121.065	4.22E+06	117.055	1.83E+06
123.044	3.69E+06	121.065	3.63E+06
181.085	4.05E+06	123.044	3.40E+06
189.037	2.68E+06	143.032	1.73E+06
193.086	2.50E+06	181.086	4.71E+06
207.047	5.50E+06	189.037	2.18E+06
227.091	1.08E+07	193.086	2.23E+06
237.073	2.34E+06	207.047	3.92E+06
253.052	2.32E+07	227.092	9.86E+06
265.067	3.06E+06	231.071	1.75E+06
269.117	4.10E+06	237.058	2.32E+06
283.078	1.28E+07	237.073	2.67E+06
290.123	2.32E+06	253.053	1.63E+07
294.102	8.54E+06	265.068	3.29E+06
299.058	5.96E+06	269.117	2.87E+06
329.083	2.26E+07	276.093	2.24E+06
330.086	2.89E+06	278.108	2.45E+06
352.123	2.47E+06	283.079	1.12E+07
359.109	3.01E+06	290.123	1.89E+06
371.137	3.28E+06	294.103	1.17E+07
375.089	1.83E+07	299.058	5.05E+06
376.092	2.56E+06	311.074	2.01E+06
405.114	8.57E+06	329.083	1.10E+07
416.138	3.75E+06	352.123	2.51E+06

446.164	1.15E+07	359.111	2.18E+06
447.168	2.51E+06	405.116	4.00E+06
451.120	6.22E+06	416.139	1.78E+06
492.170	6.45E+06	446.166	3.14E+06
497.125	2.38E+06		

115 Table S5 MS data of benzoic acid in negative ion mode. (Fig.1c)

0 ppm NH_3		0.4 ppm NH_3	
m/z	intensity	m/z	intensity
121.028	9.74E+07	121.0283	4.94E+07

Table S6 Time series of online observations. (Fig.1d, Fig.2a, Fig.2c, Fig.2e)

Time /min	Intensity-Benzoic acid-Exp.8	Intensity-Benzoic acid-Exp.10	Intensity-m/z 140	Intensity-m/z 106	Intensity-m/z 122
0	2.52E+04	6.30E+02	1.83E+04	3.30E+04	9.47E+04
1	2.75E+05	6.85E+03	3.43E+04	2.08E+05	3.13E+05
2	5.31E+05	2.98E+04	3.74E+04	5.64E+05	5.54E+05
3	8.38E+05	8.55E+04	9.74E+04	8.37E+05	8.05E+05
4	1.33E+06	9.09E+04	1.38E+05	9.41E+05	8.75E+05
5	3.47E+06	1.76E+05	2.03E+05	1.84E+06	1.16E+06
6	4.12E+06	1.73E+05	2.00E+05	1.77E+06	1.18E+06
7	5.07E+06	2.28E+05	2.16E+05	2.51E+06	1.21E+06
8	6.34E+06	2.73E+05	2.38E+05	3.07E+06	1.36E+06
9	6.25E+06	3.26E+05	2.29E+05	3.48E+06	1.65E+06
10	6.48E+06	3.91E+05	2.91E+05	3.63E+06	1.98E+06
11	8.54E+06	4.02E+05	3.33E+05	4.22E+06	2.06E+06
12	9.63E+06	4.00E+05	2.85E+05	4.39E+06	2.18E+06
13	1.14E+07	4.42E+05	3.62E+05	4.78E+06	2.32E+06
14	1.07E+07	4.73E+05	2.87E+05	5.02E+06	2.58E+06
15	1.16E+07	5.42E+05	3.09E+05	5.19E+06	2.63E+06
16	1.16E+07	5.25E+05	3.96E+05	5.43E+06	3.05E+06
17	1.17E+07	5.92E+05	3.50E+05	5.38E+06	2.93E+06
18	1.27E+07	5.87E+05	3.43E+05	5.30E+06	2.85E+06
19	1.38E+07	5.66E+05	3.20E+05	5.47E+06	3.07E+06
20	1.26E+07	6.14E+05	3.89E+05	5.71E+06	3.32E+06
21	1.36E+07	5.93E+05	3.74E+05	5.60E+06	3.37E+06
22	1.25E+07	5.79E+05	3.26E+05	5.31E+06	3.34E+06
23	1.39E+07	5.35E+05	3.52E+05	5.35E+06	3.48E+06
24	1.47E+07	6.60E+05	3.90E+05	5.62E+06	3.67E+06
25	1.37E+07	5.36E+05	3.51E+05	5.50E+06	3.71E+06
26	1.45E+07	6.44E+05	3.33E+05	5.85E+06	3.97E+06
27	1.49E+07	5.71E+05	3.52E+05	5.50E+06	3.81E+06
28	1.44E+07	6.49E+05	3.75E+05	5.80E+06	4.00E+06

29	1.41E+07	5.15E+05	3.64E+05	5.50E+06	3.93E+06
30	1.62E+07	6.74E+05	3.78E+05	5.72E+06	4.26E+06
31	1.51E+07	6.44E+05	3.29E+05	5.41E+06	4.28E+06
32	1.54E+07	6.12E+05	3.49E+05	6.02E+06	4.59E+06
33	1.53E+07	5.74E+05	3.45E+05	5.33E+06	4.19E+06
34	1.41E+07	5.52E+05	3.24E+05	5.60E+06	4.29E+06
35	1.35E+07	6.17E+05	3.84E+05	5.31E+06	4.63E+06
36	1.49E+07	5.98E+05	3.61E+05	5.56E+06	4.59E+06
37	1.49E+07	6.28E+05	3.60E+05	5.46E+06	4.64E+06
38	1.45E+07	6.07E+05	3.44E+05	5.39E+06	4.94E+06
39	1.47E+07	6.60E+05	3.36E+05	5.47E+06	4.95E+06
40	1.50E+07	5.38E+05	3.35E+05	4.95E+06	4.57E+06
41	1.59E+07	5.18E+05	4.06E+05	5.32E+06	4.97E+06
42	1.62E+07	5.49E+05	3.28E+05	5.36E+06	5.21E+06
43	1.47E+07	5.26E+05	3.17E+05	5.15E+06	4.82E+06
44	1.50E+07	6.02E+05	3.24E+05	5.29E+06	5.71E+06
45	1.52E+07	5.62E+05	3.58E+05	5.24E+06	5.37E+06
46	1.37E+07	4.97E+05	2.85E+05	5.03E+06	5.02E+06
47	1.46E+07	5.11E+05	3.06E+05	5.19E+06	5.60E+06
48	1.47E+07	5.36E+05	2.48E+05	4.76E+06	5.19E+06
49	1.52E+07	5.59E+05	3.44E+05	4.94E+06	5.62E+06
50	1.60E+07	5.74E+05	3.09E+05	5.16E+06	5.77E+06
51	1.49E+07	5.39E+05	3.42E+05	5.36E+06	5.97E+06
52	1.44E+07	5.31E+05	3.37E+05	5.00E+06	5.84E+06
53	1.53E+07	5.32E+05	3.27E+05	5.09E+06	5.65E+06

Note: Due to the large amount of data, only data with a time resolution of 1 min is displayed here.

Table S7 MS^2 data with relative abundance in the top 90%. (Fig.2b, Fig.2d, Fig.2f)

m/z 140	Intensity140	m/z 123	Intensity123	m/z 106	Intensity106	m/z 122	Intensity122
67.05	2.79E+04	79.05	3.10E+05	79.05	8.89E+05	79.05	2.60E+05
67.06	3.67E+04	79.05	5.69E+05	79.05	1.64E+06	79.05	4.83E+05
67.06	2.90E+04	79.05	8.00E+05	79.05	2.32E+06	79.05	6.89E+05
69.07	2.58E+04	79.06	6.88E+05	79.06	2.02E+06	79.06	6.04E+05
69.07	3.06E+04	79.06	4.17E+05	79.06	1.23E+06	79.06	3.69E+05
69.07	2.19E+04	79.06	1.67E+05	79.06	4.99E+05	79.06	1.52E+05
71.05	2.34E+04	96.04	2.05E+05	106.06	6.37E+05	105.03	1.41E+05
71.05	2.23E+04	96.04	3.01E+05	106.06	1.96E+06	105.03	3.79E+05
79.05	3.09E+04	96.05	2.76E+05	106.06	3.41E+06	105.03	6.36E+05
79.05	4.31E+04	96.05	1.71E+05	106.07	4.54E+06	105.03	7.77E+05
79.06	3.67E+04	105.03	2.19E+05	106.07	3.63E+06	105.04	5.73E+05
79.06	2.21E+04	105.03	5.78E+05	106.07	2.15E+06	105.04	3.23E+05
81.03	1.96E+04	105.03	9.64E+05	106.07	7.61E+05	122.06	1.27E+05
81.07	2.52E+04	105.03	1.16E+06			122.06	4.16E+05
81.07	5.05E+04	105.04	8.45E+05			122.06	7.84E+05
81.07	7.71E+04	105.04	4.71E+05			122.06	1.13E+06

81.07	7.48E+04	122.06	1.68E+05	122.06	1.01E+06
81.07	4.73E+04	122.06	5.56E+05	122.06	6.23E+05
81.07	2.17E+04	122.06	1.04E+06	122.06	2.63E+05
83.05	2.68E+04	122.06	1.49E+06		
83.05	2.58E+04	122.06	1.32E+06		
85.03	2.10E+04	122.06	8.07E+05		
93.07	2.51E+04	122.06	3.36E+05		
93.07	3.97E+04	124.04	1.76E+05		
93.07	4.12E+04	124.04	1.65E+05		
93.07	2.70E+04				
95.05	2.58E+04				
95.05	4.13E+04				
95.05	4.44E+04				
95.05	2.97E+04				
95.08	2.37E+04				
95.08	7.11E+04				
95.09	1.22E+05				
95.09	1.59E+05				
95.09	1.24E+05				
95.09	7.24E+04				
95.09	2.43E+04				
97.06	2.21E+04				
97.06	4.50E+04				
97.06	6.89E+04				
97.07	6.73E+04				
97.07	4.28E+04				
97.07	1.99E+04				
99.04	2.18E+04				
103.05	3.13E+04				
103.05	5.62E+04				
103.05	7.70E+04				
103.06	6.38E+04				
103.06	3.81E+04				
121.06	2.11E+04				
121.06	7.16E+04				
121.06	1.35E+05				
121.06	1.94E+05				
121.07	1.72E+05				
121.07	1.05E+05				
121.07	4.40E+04				
121.10	2.25E+04				
122.07	2.19E+04				
122.07	3.52E+04				

122.07	3.88E+04
122.07	2.63E+04
123.08	2.18E+04
123.08	4.08E+04
123.08	5.84E+04
123.08	5.11E+04
123.08	3.11E+04
138.02	2.80E+04
138.02	2.68E+04
139.07	4.20E+04
139.07	6.65E+04
139.08	6.84E+04
139.08	4.46E+04
139.08	2.18E+04
139.11	3.07E+04
139.11	5.23E+04
139.11	6.54E+04
139.11	4.90E+04
139.12	2.79E+04
141.05	2.01E+04
141.06	2.20E+04
141.09	4.00E+04
141.09	6.32E+04
141.09	6.52E+04
141.09	4.27E+04
141.09	2.12E+04

Table S8 The chromatograms of molecule m/z 140.071. (Fig.1 inset)

Time/min	Non-treated	Time/min	KI-treated
20.01	-2.90E+03	20.00	-1.97E+03
20.02	-1.14E+03	20.03	1.79E+03
20.03	5.90E+01	20.06	-1.22E+03
20.05	4.30E+03	20.07	8.90E+01
20.07	-3.07E+03	20.08	-1.47E+02
20.09	5.71E+02	20.10	2.90E+03
20.11	8.27E+03	20.12	1.16E+03
20.13	3.11E+03	20.13	-2.43E+03
20.14	-3.78E+03	20.14	1.56E+03
20.15	6.38E+03	20.15	1.58E+02
20.16	-3.61E+03	20.19	-8.97E+02

20.18	1.18E+03	20.20	-2.68E+02
20.19	3.19E+03	20.22	-2.45E+02
20.21	5.16E+03	20.23	2.03E+03
20.23	-1.57E+03	20.24	-2.11E+03
20.24	-1.91E+03	20.25	-3.33E+03
20.26	-1.16E+02	20.26	-2.37E+03
20.27	-2.43E+03	20.28	-9.89E+02
20.28	1.29E+03	20.30	-2.86E+03
20.30	-2.65E+03	20.31	4.14E+02
20.30	1.32E+03	20.34	-2.52E+03
20.32	-7.29E+02	20.36	2.37E+03
20.32	-3.66E+03	20.37	-2.43E+02
20.34	-1.89E+03	20.37	2.82E+03
20.36	6.59E+03	20.39	-2.79E+02
20.39	-1.35E+03	20.39	-1.33E+03
20.40	-1.37E+03	20.41	-1.71E+03
20.42	-1.54E+03	20.41	4.60E+03
20.44	6.61E+03	20.42	2.61E+03
20.45	-1.87E+03	20.43	5.36E+03
20.46	1.07E+03	20.44	-3.03E+03
20.47	-3.44E+03	20.44	-3.11E+03
20.48	-3.69E+03	20.45	4.93E+03
20.50	-8.52E+02	20.47	7.91E+02
20.53	-7.30E+02	20.48	-4.45E+03
20.59	-1.27E+03	20.49	1.07E+03
20.61	-9.37E+02	20.50	-2.12E+03
20.63	8.26E+03	20.51	-7.92E+02
20.63	-6.33E+02	20.52	8.59E+03
20.67	-2.12E+03	20.53	3.09E+03
20.68	8.59E+02	20.54	-5.24E+02
20.69	6.45E+02	20.55	-4.71E+03
20.71	2.97E+03	20.56	5.68E+03
20.72	-2.23E+03	20.59	-8.85E+03
20.73	5.52E+03	20.59	-4.77E+03
20.75	1.94E+02	20.60	1.04E+03
20.76	6.48E+02	20.61	-5.05E+03
20.77	4.91E+03	20.63	-4.59E+03

20.78	1.08E+03	20.64	1.02E+02
20.79	3.63E+03	20.65	-4.90E+03
20.82	2.10E+03	20.67	-6.59E+02
20.82	2.84E+03	20.68	7.16E+02
20.84	-1.70E+03	20.71	-1.81E+02
20.86	2.84E+03	20.71	-3.81E+03
20.88	-3.92E+03	20.73	-2.32E+03
20.94	-2.71E+03	20.73	2.68E+03
20.95	-3.86E+03	20.75	-3.55E+03
20.98	2.00E+02	20.77	-3.83E+03
20.99	-2.30E+03	20.77	8.88E+02
21.00	4.38E+03	20.79	-1.46E+03
21.01	2.79E+03	20.79	1.92E+03
21.02	2.05E+04	20.81	-2.23E+03
21.03	6.78E+04	20.81	2.31E+03
21.03	4.90E+04	20.83	8.99E+02
21.05	7.40E+04	20.85	-3.18E+03
21.05	9.03E+04	20.86	1.42E+03
21.07	1.28E+05	20.89	-5.14E+02
21.07	7.45E+04	20.90	-3.35E+02
21.09	6.09E+04	20.92	-7.76E+02
21.09	5.63E+04	20.92	3.99E+03
21.11	2.45E+04	20.93	-4.03E+03
21.11	3.20E+04	20.94	-3.18E+02
21.12	2.10E+04	20.96	1.62E+03
21.13	2.04E+04	20.97	-1.39E+03
21.14	6.27E+03	20.99	-3.95E+03
21.15	5.99E+03	20.99	-1.95E+03
21.16	8.99E+03	21.01	-2.24E+03
21.17	2.80E+03	21.02	-1.64E+03
21.18	2.51E+03	21.03	-2.65E+03
21.19	5.50E+03	21.04	9.16E+03
21.20	7.85E+03	21.04	2.74E+02
21.21	1.74E+04	21.06	-2.38E+03
21.22	7.75E+03	21.08	1.50E+03
21.23	8.37E+03	21.10	-3.35E+03
21.24	2.15E+04	21.10	-2.84E+03

21.24	2.66E+04	21.14	-5.77E+02
21.26	6.92E+03	21.21	-4.92E+02
21.26	1.37E+04	21.24	-2.59E+03
21.28	7.32E+03	21.25	3.66E+03
21.28	-1.83E+03	21.26	8.84E+02
21.30	7.50E+01	21.27	-7.52E+02
21.41	-1.63E+03	21.28	2.83E+02
21.45	6.60E+03	21.33	5.75E+03
21.45	1.81E+03	21.33	9.36E+03
21.47	1.54E+03	21.36	1.25E+03
21.53	-1.31E+03	21.37	1.73E+03
21.55	-9.94E+02	21.38	4.18E+03
21.58	-2.54E+03	21.40	2.89E+03
21.70	2.31E+03	21.42	-3.59E+03
21.81	2.62E+03	21.44	-3.08E+03
21.83	-3.07E+03	21.45	3.68E+03
21.87	-3.12E+02	21.46	5.00E+00
21.97	-3.03E+03	21.47	8.17E+03
22.12	-5.64E+02	21.48	2.12E+04
22.31	3.05E+03	21.49	1.46E+04
		21.50	1.30E+04
		21.51	1.93E+04
		21.52	-2.10E+03
		21.52	1.38E+04
		21.54	-2.23E+03
		21.56	-1.37E+02
		21.58	-2.36E+03
		21.60	-2.39E+03
		21.60	-8.55E+02
		21.62	-4.43E+03
		21.66	-4.08E+03
		21.67	-9.58E+02
		21.68	-2.98E+03
		21.71	-2.90E+03
		21.73	-1.55E+03
		21.88	-6.27E+02
		21.90	-4.97E+02

21.96	-1.97E+03
21.98	-1.76E+03
21.98	-2.19E+03
21.99	8.00E+01
22.00	-2.72E+03